applied sciences

MDPI

Article

Effect of Bond-Slip on Dynamic Response of FRP-Confined RC Columns with Non-Linear Damping

Kun Guo, Qirui Guo and Yuanfeng Wang *

School of Civil Engineering, Beijing Jiaotong University, Beijing 100044, China; 14115274@bjtu.edu.cn (K.G.); 13121021@bjtu.edu.cn (Q.G.)
* Correspondence: cyfwang@bjtu.edu.cn; Tel.: +86-10-5168-5552

Featured Application: The description of nonlinear damping theory for the dynamic analysis of FRP constrained concrete members considered on the bond slip effect of reinforcing bars provides support for subsequent seismic design.

Abstract: As a composite material, the damping energy consumption mechanism of fiber reinforced polymer-confined reinforced concrete (FRP-C RC) structure is very complex. In previous dynamic calculation models, the bond-slip effect for steel bars was often ignored, which would lead to a considerable error in the response of the FRP-C RC structures. In this paper, a new numerical model of FRP-C RC columns considering the bond-slip for steel bars is established using a zero-length element and nonlinear beam-column elements in the OpenSees software, and the results of the model are verified by experimental results. Based on the complex damping theory, the loss factor expression and nonlinear damping model of FRP-C RC columns with the bond slip effect are proposed. Finally, the dynamic response of FRP-C RC columns with nonlinear damping under harmonic load is calculated and compared with the results available in literature. The results show that the proposed model considering steel bars' bond-slip can provide better prediction for dynamic response of FRP-C RC columns and make the future seismic design of FRP-C RC columns safer.

Keywords: FRP-C RC columns; bond-slip; zero-length element; nonlinear damping; dynamic response

Citation: Guo, K.; Guo, Q.; Wang, Y. Effect of Bond-Slip on Dynamic Response of FRP-Confined RC Columns with Non-Linear Damping. *Appl. Sci.* **2021**, *11*, 2124. https://doi.org/10.3390/app11052124

Academic Editor: Tomasz M. Majka

Received: 16 January 2021
Accepted: 24 February 2021
Published: 27 February 2021

1. Introduction

FRP (Fiber Reinforced Polymer) materials have been widely used in various civil engineering fields due to their superior properties such as light weight, high strength, and corrosion resistance [1–4], especially in some seismic strengthening of concrete structures [5–7]. FRP-confined reinforced concrete (FRP-C RC) columns show superior seismic performance [8–12].

In recent years, many static behavior studies on subjects such as axial compression performance and various calculation models of FRP-confined concrete have been conducted. Ozbakkaloglu et al. [13] assessed the performances of 88 existing prediction models by establishing a test database of 730 FRP-confined concrete cylinders tested under monotonic axial compression, and indicated Lam and Teng 2003 model [14] as one of the top performing models. Nevertheless, in the dynamic analysis of FRP-confined concrete, to simplify the engineering calculation, the damping coefficient is generally defined as a constant [15]. For instance, Ozcana et al. [16] and Balsamo et al. [17] adopted the constant damping ratio of concrete materials in studying the seismic performance of FRP-confined concrete columns. To the best of the author's knowledge, there are few researches on nonlinear damping of FRP-C RC materials. Su et al. [18] conducted an experimental and numerical investigation to study the cyclic behavior and the energy dissipation of CFRP-confined square RC columns. Wang and Li [19] simulated the hysteretic behaviors of two tested FRP-confined circular columns and proposed a six parameter stress-dependent damping model. Based on a damping-stress relation, Li et al. [20] developed an iterative scheme for

the computations of the non-linear damping and dynamic response of FRP-C RC columns at any given harmonic exciting frequency.

In fact, as a composite material, the damping and energy dissipation mechanism of FRP-C RC materials are very complex. A constant damping ratio can't truly represent the complex damping characteristics of actual structures. In addition, it is unreliable if the damping ratio of the FRP-C RC composite structure is still the same as that of ordinary concrete structure. In conclusion, it is necessary to further explore the damping and dynamic characteristics of FRP-C RC materials and structures.

On the other hand, there are many failure modes of FRP-C RC members under loading, including "premature" tensile failures of FRP jacket studied by Zinno et al. [21], concrete cover spalling, reinforcement buckling described by Lignola et al. [22], and bond-slip stated by Zhao and Sritharan [23], in addition to the bearing capacity failure. Lignola et al. [24] have presented an analytical model to directly evaluate the FRP strain efficiency factor as the strain ratio between the effective FRP hoop strain at failure and the flat coupon test outcomes. However, this paper focuses on capturing the bond slip due to strain penetration along fully anchored bars into FRP-confined concrete columns footings and assumes that FRP fails when hoop strain in the jacket reaches its ultimate tensile strain determined according to flat coupon tests. The bond-slip between steel bar and concrete has influences on cyclic performance of reinforced concrete (RC) structures [25–27]. The research of Verderame et al. [28,29] indicated that the deformation component associated with bar slippage in elements with plain bars may contribute to 80–90% of the elements' overall deformability. For a reinforced concrete column subjected to seismic load, localized inelastic deformation easily occurs at the column foot where the stress gradient is higher, due to reinforcement slip. This slip results from strain penetration along a portion of the fully anchored bars into the adjoining concrete members [30]. In previous analysis, Otani [31] used nonlinear rotational springs at the end of beam-column elements to include the member end rotation due to strain penetration effects, which cause large computation and low precision problems due to the empirical nature. In order to simplify the calculation, the steel bars' bond-slip effect is often ignored in the structural analysis. However, in subsequent studies neglecting the effects of bond-slip will lead to smaller prediction of lateral deformation and overestimation of energy dissipation under cyclic load and curvature of skeleton curve [32]. Until Zhao and Sritharan [33] introduced a hysteretic model for the reinforcing bar stress versus slip response using a zero-length section element for dealing with the member end rotation in the RC column foot. Nevertheless, as far as the author knows, there is almost no research conducted on the influence of localized steel bond-slip on of FRP-C RC columns based on nonlinear damping theory.

Given the FRP confinement effect and the importance of reinforced slip on the structural seismic analysis, it is necessary to consider the influence of bond-slip on energy dissipation and damping performance of FRP-C RC columns. For establishing a nonlinear damping model considering localized steel bond-slip for FRP-C RC column, this paper mainly carries out the following works: (1) A zero-length section element available in the OpenSees [34,35] is introduced to simulate the steel bars' bond slip of FRP full-confined RC columns; (2) and the regression analysis of unit energy dissipation formula is conducted to redefine the damping ratio of FRP-C RC columns; and (3) finally, the time-history analysis of FRP-C RC columns considering localized steel bond-slip under harmonic loads is conducted.

2. Numerical Model of FRP-C RC Columns Considering Bond-Slip Effect

2.1. Modeling Method for Bond-Slippage

As stated by Mazzoni et al. [34], the strain penetration effects or the fixed end rotations may be accounted accurately by the zero-length section element available in the OpenSees. A zero-length section element is a fiber discretization of the cross section of a structural member, which is assumed by Zhao and Sritharan [33] to have a unit length such that the section deformation (for example, curvature) is equal to the element deformation (for

example, rotation). The unit length assumption also implies that the material model for the steel fibers in the section element would represent the bar slip instead of strain for a given bar stress. By attaching a zero-length element at the end of a beam-column element instead of a spring element, the bending deformation and sliding deformation of the element can be separated, as shown in Figure 1. A new node j is added at the bottom of the beam-column element and the node i and j (the distance between Node i and j is zero) are connected by a zero-length element which is used to simulate the bond-slip of reinforcement in reinforced concrete members.

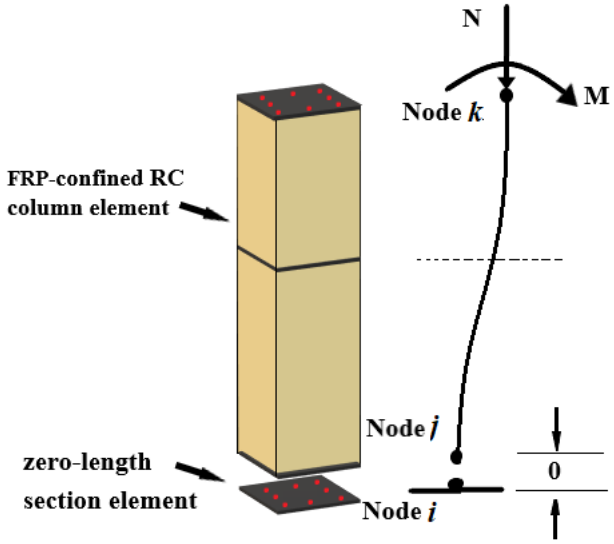

Figure 1. Fiber-based modeling of strain penetration effects.

It should be emphasized that (1) the zero-length section element and the adjacent beam-column element have the same fiber division, steel bar, and concrete configuration; (2) the stress-strain relationship of reinforcement is used for the FRP-C RC beam-column element, and the stress-slip relationship of reinforcement is used for the zero-length element; (3) the research object of this paper is the fully wrapped FRP-C RC columns; (4) and the restraining effect of FRP is considered, while the double restraint effect of FRP and stirrup is neglected.

2.2. Material Constitutive Models and Loading-Unloading Criteria

To establish a finite element analysis model, the stress-strain relationship of materials and the element type must be determined. In this paper, finite-element models for FRP-C RC element and zero-length element are established, as shown in Figure 1.

2.2.1. FRP-C RC Column Element

In this paper, the concrete compression skeleton curve model selected is the Kent-Park model (refer to Concrete 01 model, in the OpenSees program) improved by Scott et al. [36]. The Karsan-Jirsa model [37] is used to reflect the actual stress-strain hysteresis relationship of concrete under repeated loads.

The stress-strain relationship of FRP-C RC columns adopts the Lam-Teng model proposed by Lam and Teng [14,38]. For the specific mathematical expressions and parameter values of the model, please refer to references [14,38].

The Menegotto-Pinto model modified by Filippou et al. [39] is used as the material constitutive model for longitudinal reinforcement of FRP-C RC column.

2.2.2. Zero-Length Section Element

As illustrated by Zhao and Sritharan [33], the bond-slip model of reinforcement in zero-length element is represented by a stress-slip relationship, which can be described by

an elastic straight line for the elastic stage and a curved section for the post-yield region. The schematic diagram is shown in Figure 2.

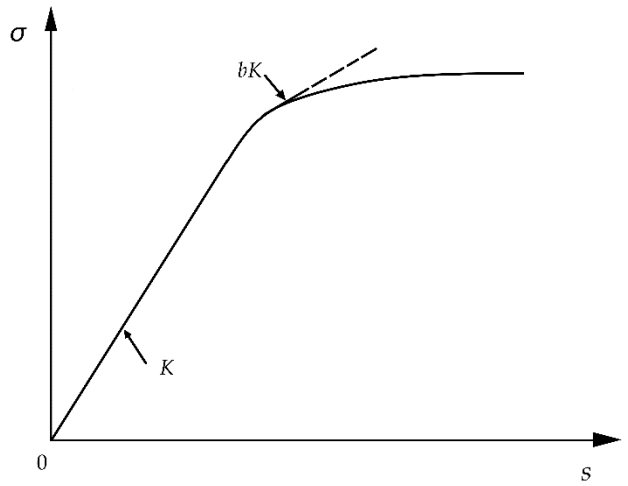

Figure 2. The bar stress versus loaded-end slip relationship for the zero-length element.

The stress-slip curve relations are described as follows:

$$\sigma = Ks \text{ for } 0 \le s \le s_y \tag{1}$$

$$\sigma = \widetilde{\sigma} \times \left(f_u - f_y\right) + f_y \text{ for } s_y \le s \le s_u \tag{2}$$

$$\widetilde{\sigma} = \frac{\frac{\widetilde{s}}{\mu - \widetilde{s}}}{\sqrt[R_e]{\left(\frac{1}{\mu \times b}\right)^{R_e} + \left(\frac{\widetilde{s}}{\mu - \widetilde{s}}\right)^{R_e}}} \tag{3}$$

$$\widetilde{s} = \frac{s - s_y}{s_y} \tag{4}$$

$$\gamma = \frac{s_u - s_y}{s_y} \tag{5}$$

where, k is the slope in the elastic region; $\widetilde{\sigma}$ and $\widetilde{s}$ are the normalized bar stress and slip, respectively; f_y and f_u are the yield and ultimate strength of the steel reinforcing bar; γ is the ductility coefficient; b is the stiffness (K) reduction factor; s_y and s_u are the loaded-end slips when bar stresses are f_y and f_u, respectively; $\mu = (s_u - s_y)/s_y$ is the ductility coefficient; and the value of factor R_c is taken as 1.01.

By simulating the pull-out test data of the steel, Zhao and Sritharan [33] obtained a regression empirical formula of s_y.

$$s_y = 2.54 \times \left[\frac{d_b}{8437} \times \frac{f_y}{\sqrt{f_c'}} \times (2\alpha + 1)\right]^{\frac{1}{\alpha}} + 0.34 \tag{6}$$

where α is the parameter for the local bond-slip relation; d_b is the bar diameter; and f_c' is the concrete compressive strength.

The limited test information available in the literature [33] indicated that $30s_y \le s_u \le 40s_y$ and $0.3 \le b \le 0.5$ would be appropriate. In this study, $s_u = 35s_y$, α and b are taken as 0.4 and 0.5 separately. The hysteresis curve schematic diagram of the bond-slip model is shown in Figure 3.

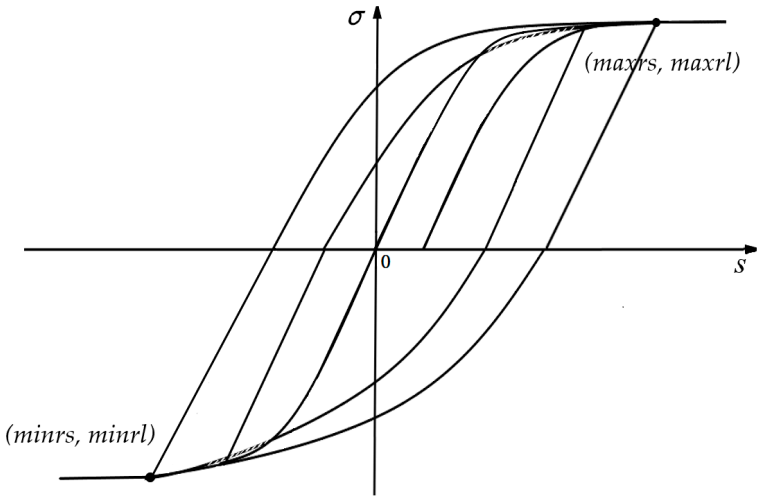

Figure 3. Hysteretic model schematic diagram for the bar stress vs. loaded-end slip relationship.

A reloading path of this model is defined in the following Equations (7)–(10):

$$\sigma = \sigma^* maxrl \text{ or } \sigma = \sigma^* minl \tag{7}$$

$$\sigma^* = \frac{\frac{s^*}{s_{uy}-s^*}}{\left[\left(\frac{1}{s_{uy}}\right)^{R_c} + \left(\frac{s^*}{s_{uy}-s^*}\right)^{R_c}\right]^{\frac{1}{R_c}}} \tag{8}$$

$$s^* = \frac{s - rsvg}{s_y'} \tag{9}$$

$$s_{uy} = \frac{maxrl - rsvg}{s_y'} or \frac{minrl - rsvg}{s_y'} \tag{10}$$

where, σ^* is the bar stress ratio; s^* is the slip ratio; s_{uy} is the stress limit ratio; s_y' is the slip recovered elastically as determined by the return stress divided by the initial slope (K); the variable (maxrs, maxrl) denotes the maximum bar stress and the corresponding slips; and the variable (minrs, minrl) denotes the minimum bar stress and the corresponding slips; the variable ($rsvg$, 0) is the intersection between the straight unloading/reloading path and the s-axis; and R_c is the coefficient defining the shape of the reloading curve. R_c is taken as 1.0.

The Kent-Scott-Park model proposed by Scott et al. [36] is still used for concrete in the zero-length section element, and the corresponding hysteretic criterion can be referring to the Concrete 01 model in the OpenSees.

2.2.3. Verification of the Proposed Model of FRP-C RC Columns Considering Bond-Slip

After determining the material constitutive relations and corresponding hysteretic criterions, the nonlinear beam and column element based on the flexibility method and zero-length element considering bond-slip of steel bars are available for FRP-C RC columns modeling. Firstly, we adopt a load control to apply axial load on the top of the column while using a displacement control scheme for cyclic load at the horizontal position, and each load increment step carries out a cyclic iteration until convergence. The iterative algorithm of Newton-Raphson is adopted to control convergence. Here, the simulation results of FRP-C RC square and circular columns are separately compared with the experimental results provided by Su et al. [18] and Yoneda [40], as shown in Figure 4.

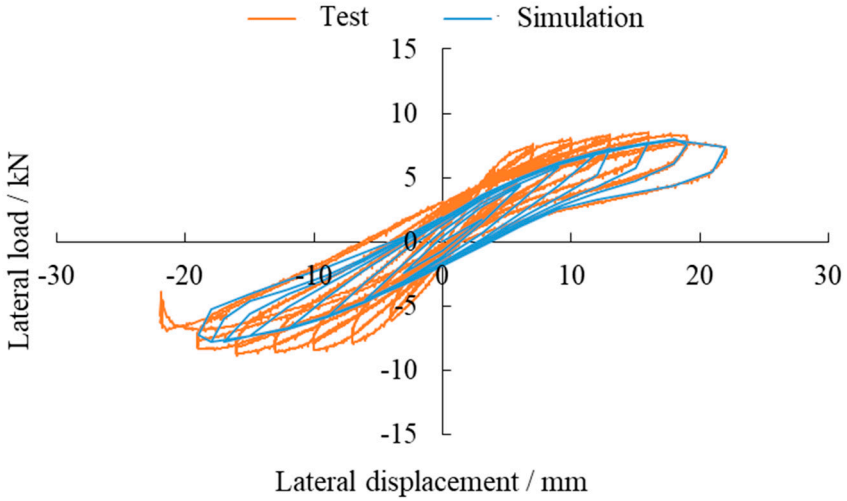

(**a**)

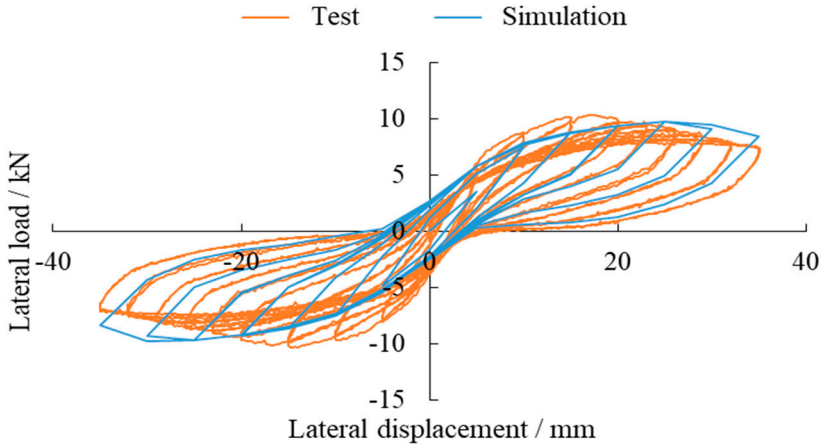

(**b**)

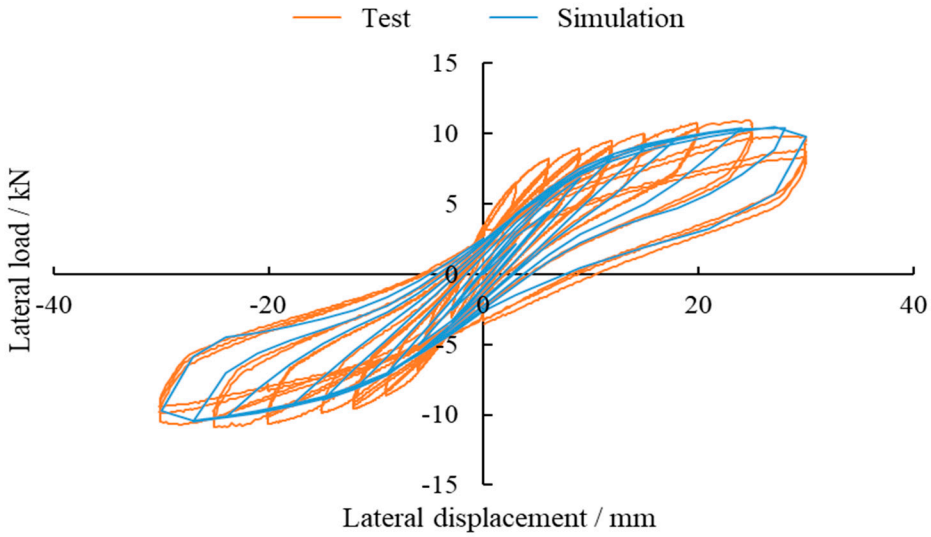

(**c**)

Figure 4. *Cont.*

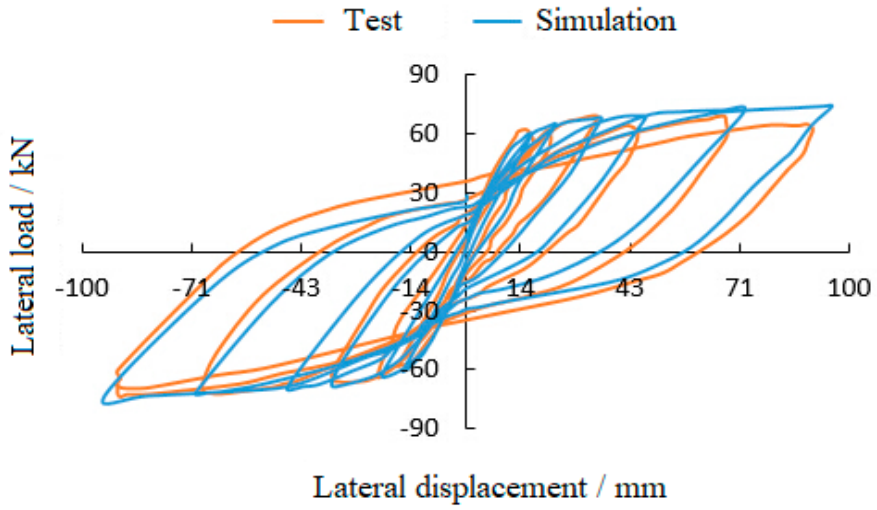

(**d**)

Figure 4. The results of test in literatures [18] and [40] versus numerical results for hysteretic Scheme 1. (**a**) AR-1, (**b**) Scheme 3. (**c**) Specimen BR-1, and (**d**) Tall Circular Column specimen.

It can be seen from Figure 4 that almost all the simulated hysteresis curves show a more significant pinching effect. Whether the square columns [18] or circular columns [40], the simulated hysteresis curves are in good agreement with the experimental hysteretic curves, especially for the square specimens coated with a layer of FRP, such as AR-1 and BR-1.

In addition, the reliability of the proposed model can be proved from the perspective of energy dissipation by comparing the areas of hysteresis loops under different lateral drift rates. Here, we still take AR-1 and BR-1 square specimens [18] and the tall circular column specimen [40] as examples, the energy dissipation versus the lateral drift rate ($\mu' = \frac{\Delta}{L}$, where Δ represents the average of the forward and reverse peak point displacements of a certain cycle, L indicates the vertical height of the specimen loading point to the upper surface of the bottom beam) curves of the specimens are evaluated, and the specific results are shown in Table 1.

Table 1. Comparison of tests data and numerical results for energy dissipation of fiber reinforced polymer-confined reinforced concrete (FRP-C RC) columns.

Specimen	Compare the Item	Value of Calculated Results				
AR-1 [18]	Lateral drift rate	0.002	0.005	0.009	0.011	0.013
	Tests data	5.16	31.36	76.85	118.66	157.52
	Numerical results	5.03	27.58	70.63	108.28	147.83
	Relative error (%)	2.52	12.05	8.09	8.75	6.15
BR-1 [18]	Lateral drift rate	0.002	0.005	0.009	0.014	0.018
	Tests data	3.30	30.65	83.28	191.90	288.12
	Numerical results	3.15	28.37	77.32	185.89	267.95
	Relative error (%)	4.55	7.44	7.16	3.13	7.00
Tall circular column [40]	Lateral drift rate	0.002	0.0033	0.046	0.006	0.073
	Tests data	70.83	445.38	896.75	1379.16	1882.67
	Numerical results	65.1	422.35	810.92	1301.75	1743.83
	Relative error (%)	8.09	5.17	9.57	5.61	7.37

Note: The value unit of test data and numerical results in Table 1 are kN·mm.

For AR-1 and BR-1 square specimens, the calculated values of the proposed model in this paper fit better to the test results. The relative errors of the simulation and test results are less than 10%, except for the case of the AR-1 specimen with a lateral drift rate at

0.005, the relative error is 12.05%. Take the AR-1 square specimen as an example; when the lateral drift rate is 0.09, the energy dissipation value of test data and numerical result are 76.85 kN·mm and 70.63 kN·mm, respectively, and the relative error is 8.09%. Similarly, for the tall circular column specimen, the energy dissipation value of the proposed model is close to the test value at every lateral drift rate, and all the relative errors are less than 10%.

The above analysis results show that the proposed model of FRP-C RC columns considering bond-slippage is reasonable for hysteretic dissipation energy analysis.

3. The Unit Energy Dissipation

3.1. Definition

To study the dynamic response of FRP-C RC columns based on a nonlinear damping theory, this paper introduces a damping calculating method with the so-called loss factor proposed by Lazan [41], given by

$$\eta = \frac{W}{\pi \int_V \frac{\sigma^2}{E} dV} = \frac{W}{\pi k' {u_0}^2} \tag{11}$$

$$W = \int_V \Delta U(\sigma) dV = \pi c \omega {u_0}^2 \tag{12}$$

where, η is the loss factor, W is the energy dissipation per cycle for the total volume (V) of structure member, f'_{cu} is the stress amplitude, ΔU is the unit energy dissipation, c is the damping coefficient, u_0 is the displacement amplitude, ω is the exciting frequency, and k' is the stiffness of the system.

Lazan [41] found that the damping energy dissipation of materials in the hysteresis process is mainly related to the maximum stress amplitude. Moreover, the relationship between the unit energy dissipation (ΔU) and maximum stress amplitude ($\sigma_{\max}$) is obtained as follows:

$$\Delta U(\sigma) = J\sigma^m \tag{13}$$

where, J and m are constants determined according to experiments.

Wang and Li [19] proposed a five-element nonlinear regression formula of the unit energy dissipation of FRP-C RC columns, in the form of the following equation:

$$\Delta U(\sigma, \rho, \gamma, n, f'_{cu}) = a \times \sigma^b \times (1+\rho)^c \times (1+\gamma)^d \times (1+f'_{cu})^e \times (1+f \times n + g \times n^2) \tag{14}$$

where, ρ is the longitudinal reinforcement ratio, $\rho = A_s / A_{column}$, with A_s is the cross-sectional area of longitudinal reinforcement and A_{column} is the effective cross-sectional area of the column; γ is the FRP volume ratio, $\gamma = 4t_f / D$, with t_f is the thickness of FRP one-layer and D is the diameter of a cylinder or the length of a square column; n is the axial compression ratio; and f'_{cu} is the strength of concrete.

In the process of calculating hysteretic energy dissipation of materials, a specific command (Recorder Element-file ele1sec1Stress-Strain. Out-time-ele1 section1 fiber $y $z < $mat ID > Stress-Strain) provided by the OpenSees can obtain the stress-strain relationship. However, under the action of the horizontal reciprocating forces, the theoretical maximum stress amplitude ($\sigma_{\max}$) appears at the bottom of the column, and the integral point cannot be defined on the zero-length section element. As a result, the above command in the OpenSees does not capture the stress-strain relationship on a zero-length element. Therefore, we propose a method to calculate the energy dissipation by using the maximum horizontal displacement amplitude ($S_{\max}$) at the top of the column to replace the maximum stress amplitude ($\sigma_{\max}$), with the form of the following equations:

$$\sigma_{\max} = f(S_{\max}) = a + b \times S_{\max} + c \times {S_{\max}}^2 + \cdots\cdots + z \times {S_{\max}}^{n+1} + \theta(S_{\max}) \tag{15}$$

$$\Delta U(S_{\max}, \rho, \gamma, n, f'_{cu}) = a^* \times f(S_{\max})^{b^*} \times (1+\rho)^{c^*} \times (1+\gamma)^{d^*} \times (1+f'_{cu})^{e^*} \times (1+f^* \times n + g^* \times n^2) \tag{16}$$

where a, b, c . . . , a^*, b^*, ... are undetermined constants.

3.2. Calculation Models

In order to establish the relationship between the unit energy dissipation and multiple variable parameters, the validated model in Section 2 and the FRP-C RC columns tested by Tao and Yu [42] are utilized, as shown in Figure 5. Where, the FRP-confined circular columns are of 150 mm diameter by 1.5 m in height, and the FRP-confined square columns are of 200 mm wide by 0.6 m in height. For all test columns, the yield strength and elastic modulus of longitudinal reinforcement are 366 MPa and 196 GPa, respectively; the thickness and tensile strength of one-layer FRP are selected as 0.17 mm and 4212 MPa, respectively; the ultimate strain is set at 0.0167.

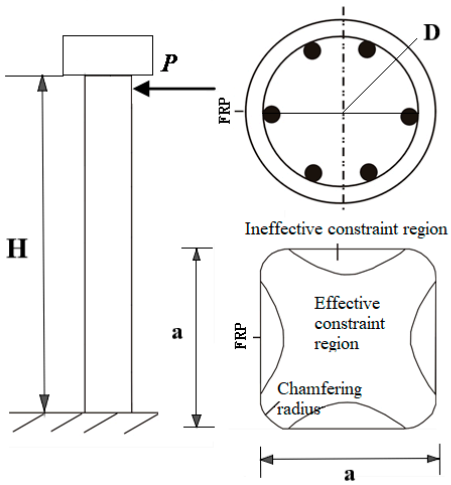

Figure 5. Section shape and loading form of FRP-C RC columns.

Four parameters are studied, and only the maximum horizontal displacement amplitude (S_{max}) parameter at a time is considered as a variable, as shown in Table 2.

Table 2. Case study parameter matrix of FRP-C RC material energy dissipation analysis.

Parameters				
Cross section type	Concrete strength f'_{cu}/MPa	Reinforcement ratio ρ/%	FRP volume γ/%	Axial compression ratio/n
Circular column	30, 40, 50	2.67 ((Φ = 10 mm)), 5.23 (Φ = 12 mm), 8.64 (Φ = 18 mm)	0.45 (1 layer), 0.91 (2 layer), 1.36 (3 layer)	0.1, 0.2, 0.3
Square column	30, 40, 50	1.56 (Φ = 14 mm), 2.58 (Φ = 18 mm), 3.85 (Φ = 22 mm)	0.32 (1 layer), 0.96 (3 layer), 1.61 (5 layer)	0.1, 0.2, 0.3

Note: Φ is the diameter of the longitudinal reinforcement.

3.3. Establishment of the Unit Energy Dissipation Formula

For the random combination of the four parameters in Table 2, 81 different calculation schemes can be derived by OpenSees for circular column and square column, respectively. Using function drawing software Origin, nonlinear integration of the hysteretic curve under each condition above is carried out. By calculating the area enclosed by the time-delay loop with different horizontal displacement amplitude and dividing by the volume of the component, the energy dissipation per unit volume of the FRP-C RC columns with different parameter combinations can be obtained.

Therefore, establishing a calculation formula of the energy dissipation per unit volume is a five-element (the maximum horizontal displacement amplitude, concrete strength, reinforcement ratio, FRP volume, axial compression ratio) nonlinear regression problem. A method of fixing other parameters and examining a single parameter is adopted to analyze

its influence on the whole curve one by one. The Statistical Program for Social Sciences (SPSS) is used to conduct a regression analysis for each single parameter and material constant until achieve a unified expression by combining these formulas.

Due to the limit of the length of the paper, the effects of the concrete strength and reinforcement ratio on the unit energy dissipation of FRP-C RC circular columns and square columns are only plotted in Figure 6a–d.

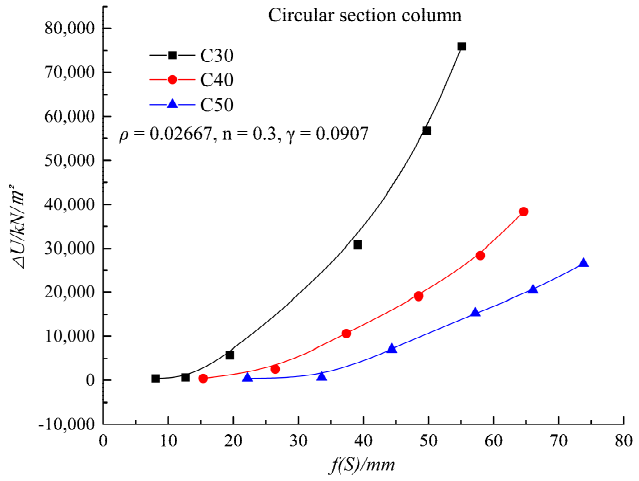

(**a**)

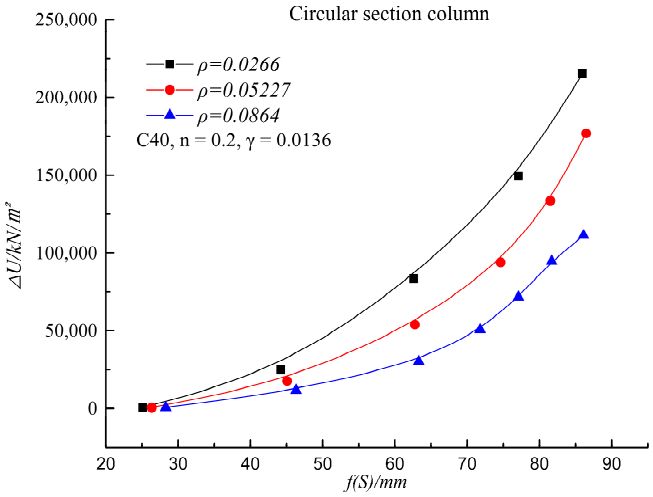

(**b**)

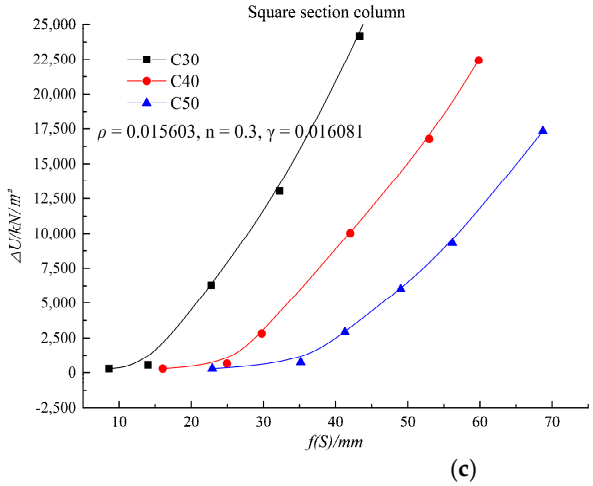

(**c**)

Figure 6. *Cont.*

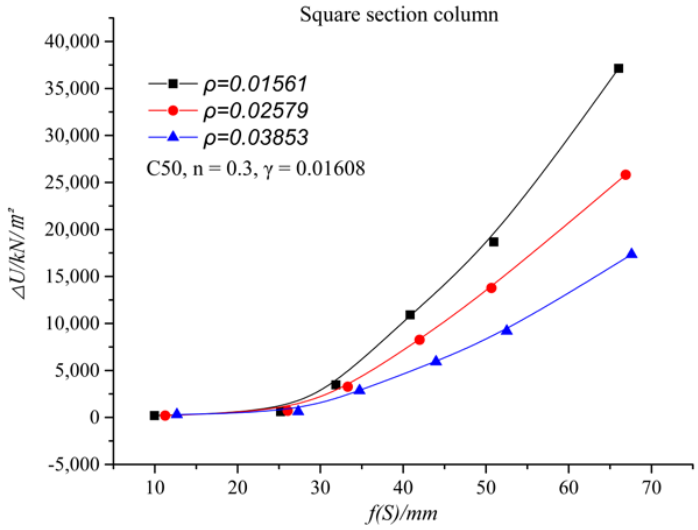

(**d**)

Figure 6. The relation between the unit energy dissipation and maximum stress f(S) of the FRP-confined columns: (**a**) circular section (ρ = 0.02667, n = 0.3, γ = 0.00907); (**b**) circular section (C40, n = 0.2, γ = 0.0136); (**c**) rectangular section (ρ = 0.015603, n = 0.3, γ = 0.016081); and (**d**) rectangular section (C50, n = 0.3, γ = 0.01608).

After the above calculation and analysis, the formulas of the energy dissipation per unit volume of FRP-C RC circular columns and square columns considering bond-slippage can be obtained, as shown in the following Equations (17) and (18).

For circular columns:

$$\Delta U(S,\rho,\gamma,n,f'_{cu}) = a^* \times f(a + b \times S + c \times S^2 + d \times S^3)^{b^*} \times (1+\rho)^{c^*} \times (1+\gamma)^{d^*} \times (1+f'_{cu})^{e^*} \times (1 + f^* \times n + g^* \times n^2) \quad (17)$$

where, a^* = 1.095, a = 9,531,170.569, b = 58,665.047, c = −117,075.512, d = 1280.522, b^* = 1.146, c^* = 18.073, d^* = 33.528, e^* = 0.359, f^* = 40.162, g^* = −100.427, the R-squared value of the regression results is 0.942.

For square columns:

$$\Delta U(S,\rho,\gamma,n,f'_{cu}) = a^* \times f(a + b \times S + c \times S^2 + d \times S^3 + e \times S^4)^{b^*} \times (1+\rho)^{c^*} \times (1+\gamma)^{d^*} \times (1+f'_{cu})^{e^*} \times (1 + f^* \times n + g^* \times n^2) \quad (18)$$

where, a^* = 2.818, a = 646,248.526, b = −853010.979, c = 204,865.377, d = 1895.954, e = 0.814, b^* = 1.526, c^* = 35.627, d^* = 2.121, e^* = 0.014, f^* = −0.008, g^* = −0.752, the R-squared value of the regression results is 0.996.

4. Effect of Bond-Slip on the Dynamic Response of the FRP-C RC Columns

Using this validated numerical model in Section 2 and the unit energy dissipation in Section 3, a new nonlinear damping expressions of FRP-C RC columns is presented in Section 4. Finally, utilizing the Newmark-β integration method in the OpenSees, the dynamic responses of FRP-C RC columns considering bond-slip of steel bars under harmonic loads can be conducted, and corresponding results are compared with the outcomes calculated by Li [43] without considering the bond-slip of reinforcement.

4.1. Loss Factor

Substituting Equations (12) and (15)–(18) into Equation (11) reduces the new loss factor η expression as follows:

$$\eta = \frac{E}{\pi} \cdot \frac{\int_V \Delta U(S) dV}{\int_V f(S)^2 dV} \quad (19)$$

where, E is the elastic modulus of composite materials of FRP-C RC columns.

For circular columns, the loss factor η can be calculated as

$$\eta = \frac{E}{\pi} \times \frac{\int_V 1.095 \times f(9.53 \times 10^6 + 5.87 \times 10^4 \times S - 1.17 \times 10^5 \times S^2 + 1.28 \times 10^3 \times S^3)^{1.146} \times (1+\rho)^{18.073} \times (1+\gamma)^{33.528} \times (1+f'_{cu})^{0.359} \times (1+40.16 \times n - 100.427 \times n^2) dV}{\int_V f(9.53 \times 10^6 + 5.87 \times 10^4 \times S - 1.17 \times 10^5 \times S^2 + 1.28 \times 10^3 \times S^3)^2 dV} \quad (20)$$

For square columns, the loss factor η can be calculated as

$$\eta = \frac{E}{\pi} \times \frac{\int_V 2.818 \times f(6.46 \times 10^5 - 8.53 \times 10^5 \times S + 2.049 \times 10^5 \times S^2 + 1.895 \times 10^3 \times S^3 + 0.814 \times S^4)^{1.526} \times (1+\rho)^{35.627} \times (1+\gamma)^{2.121} \times (1+f'_{cu})^{0.014} \times (1 - 0.008 \times n - 0.752 \times n^2) dV}{\int_V f(6.46 \times 10^5 - 8.53 \times 10^5 \times S + 2.049 \times 10^5 \times S^2 + 1.895 \times 10^3 \times S^3 + 0.814 \times S^4)^2 dV} \quad (21)$$

4.2. Dynamic Equilibrium Equations with Nonlinear Damping

In this paper, the influence of the nonlinear damping property of the structure under harmonic load on the vibration is analyzed. In viscous damped systems, the dynamic equilibrium equations of FRP-C RC columns under harmonic load are as follows:

$$m\ddot{u} + c\dot{u} + ku = P_0 \sin \overline{\omega} t \quad (22)$$

$$c = 2m\xi\omega \quad (23)$$

The displacement u as general solutions of Equation (22) takes the following form:

$$u(t) = \exp(-\xi\omega t)[u(0)\cos\omega_D t + (\frac{\dot{u}(0) + \xi\omega_n u(0)}{\omega_D})\sin\omega_D t] + \frac{P_0}{\kappa}[(1-\beta^2)^2 + (2\xi\beta)^2]^{-1} \times [(1-\beta^2)\sin\overline{\omega}t - 2\xi\beta\cos\overline{\omega}t] \quad (24)$$

In order to obtain the nonlinear damping ratio ξ, combined with the theory of complex damping, the energy dissipation E_D of hysteretic damping in a vibration cycle is:

$$E_D = \pi\dot{\eta}ku_0^2 \quad (25)$$

Based on the principle of energy equivalence, the calculation formula of equivalent damping ratio ξ_{eq} is given by:

$$\xi_{eq} = \frac{E_D}{2\pi(\omega/\omega_n)ku_0^2} \quad (26)$$

Substituting Equation (25) into Equation (26) reduces the relation between the equivalent viscous damping ratio ξ_{eq} and the complex damping coefficient $\dot{\eta}$ as follows:

$$E_D = \pi\dot{\eta}ku_0^2 \quad (27)$$

As stated by Wang and Li [19], the loss factor η is equal to the complex damping coefficient $\dot{\eta}$. The loss factor η is calculated by Equation (20).

In summary, through the derivation of the above formulas, the nonlinear damping ratio in the dynamic equation is redefined.

4.3. Seismic Simulation Results and Discussion

Based on the OpenSees platform, the dynamic responses of the FRP-C RC circular and square columns considering bond-slip of steel bars are calculated by applying unidirectional and bidirectional harmonic loads.

The specific algorithm refers to the literature [43] is as follows: The cross-section is evenly divided into 5 integral control points along the column height, the initial damping ratio of the first two modes is set as 0.02. The peak values of harmonic load acceleration are both selected as 0.1g in horizontal and vertical directions. The period of simple harmonic wave is 0.35 s, the duration is 1.35 s, the calculation time is set as 20 s, and the sampling period is 0.01 s.

The time-history responses of the column head displacement are calculated, and compared with the calculated results neglecting the bond-slip of reinforcement of reference [43]. The results are plotted in Figures 7–10.

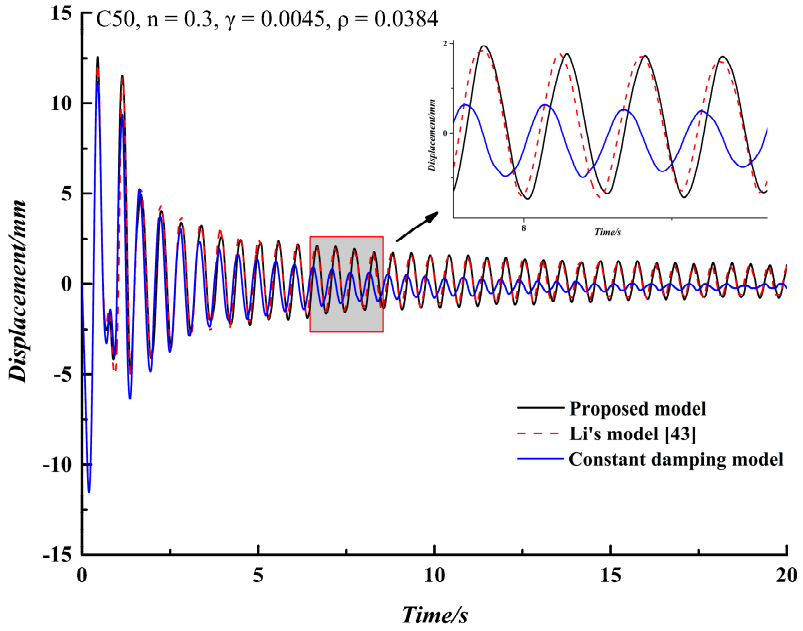

Figure 7. The column head displacement response of FRP-C RC columns with circular section under uniaxial harmonic load (C50, n = 0.3, γ = 0.0045, ρ = 0.0384).

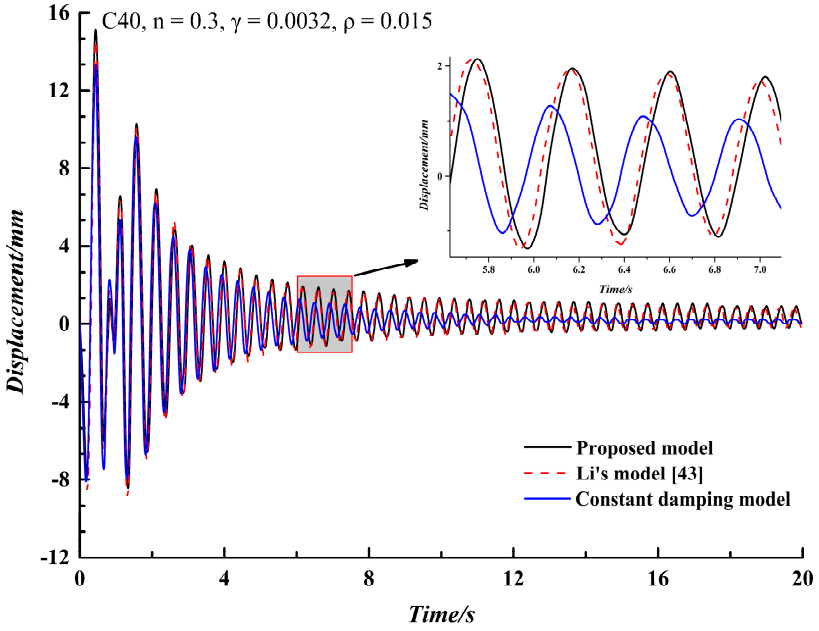

Figure 8. The column head displacement response of FRP-C RC columns with rectangular section under uniaxial harmonic load (C40, n = 0.3, γ = 0.0032, ρ = 0.015).

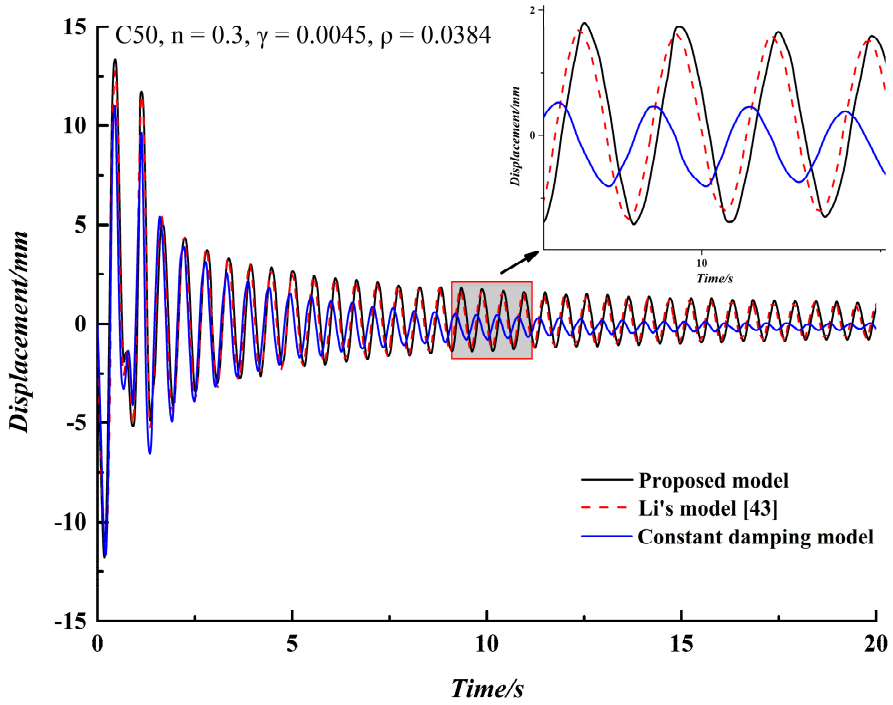

Figure 9. The column head displacement response of FRP-C RC columns with circular section under biaxial harmonic load (C50, n = 0.3, γ = 0.0045, ρ = 0.0384).

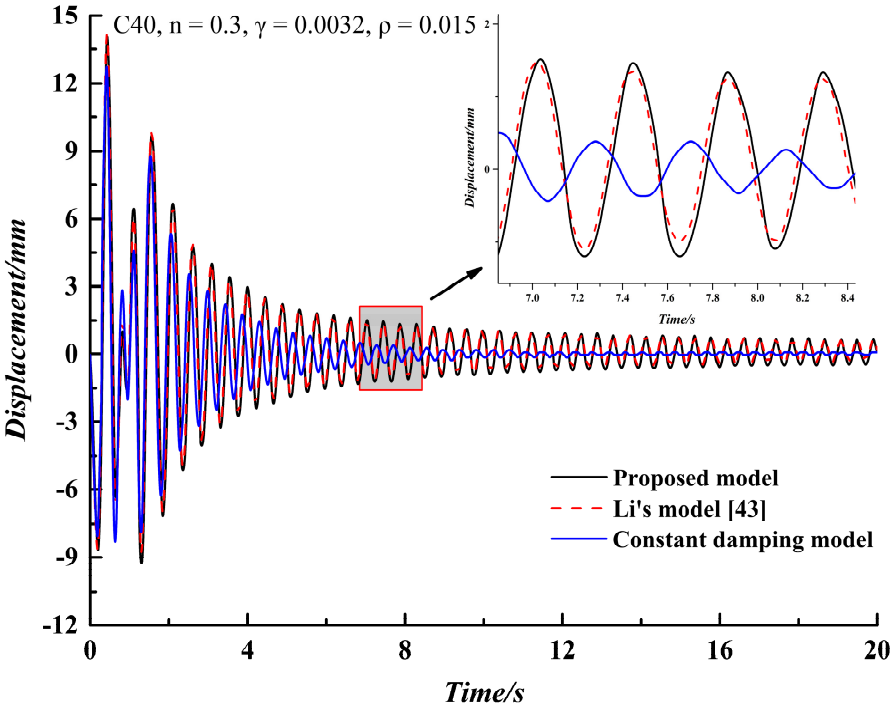

Figure 10. The column head displacement response of FRP-C RC columns with rectangular section under biaxial harmonic load (C40, n = 0.3, γ = 0.0032, ρ = 0.015).

It should be noted that in the following figures: The nonlinear damping model proposed by this paper considered the bond slippage (i.e., Proposed model; the Li's nonlinear damping model does not consider the bond slippage (i.e., Li's model); the constant damping model does not account for the bond slippage (i.e., Constant damping model).

Figures 7–10 show that under the uniaxial and biaxial harmonic loads, for two different nonlinear damping models (e.g., the proposed model and Li's model [43]), the trend of

displacements with time is almost consistent. The displacement responses of the proposed model by this paper considering the bond slip-page are slightly larger than those of Li's model. More importantly, the calculated results of the column top displacements with two time-varying damping ratios are both greater than that with constant damping. In addition, the displacement response calculated by the constant damping model decays obviously faster with time increasing. In addition, the displacement responses of biaxial harmonic loads are smaller than that of uniaxial harmonic loads.

To illustrate this further, the comparison results of the maximum of column top displacement in the above three models are shown in Table 3.

Table 3. The comparison results of the maximum of column top displacement in the above three models.

Cross Section Form	External Load	D_1/mm	D_2/mm	D_3/mm	$(D_1–D_2)/D_2$	$(D_1–D_3)/D_3$
Circular column	Uniaxial harmonic load	13.1	12.5	11.2	4.80%	16.96%
	Biaxial harmonic load	12.9	12.3	11.6	4.87%	11.21%
Square column	Uniaxial harmonic load	15.9	14.8	13.0	7.43%	22.31%
	Biaxial harmonic load	15.6	14.7	12.8	6.12%	21.88%

Note: D_1 is the maximum of column top displacement by the proposed model; D_2 is the maximum of column top displacement by Li's model; D_3 is the maximum of column top displacement by the constant damping model.

For the circular columns, the column top maximum displacement of the proposed damping model is almost 5% larger than that of the Li's model, and 15% larger than that of the constant damping model. Similarly, for the square columns, the column top maximum displacement of the proposed damping model is almost 7% larger than that of the Li's model, and 21% larger than that of the constant damping model.

According to the above analysis results, the main reasons are as follows:

(1) Firstly, because the nonlinear damping model considering the stress/displacement and amplitude of change on the influence of damping values change, even in the elastic stage of material, the damping ratio will be increased with the increase of amplitude, which conform to the material when the forced vibration energy dissipation and reflect the damping performance of materials in vibration process [43];

(2) secondly, once FRP-C RC columns are considered the bond slip of longitudinal reinforcement, the component of energy dissipation and stiffness are all in a certain degree of lower. Hence, in the time history analysis, the displacement response of the proposed model by this paper compared to the other two model results is larger. That means that if the influence of longitudinal reinforcement bond-slip is taken into account, it can improve the component's safety in the structural design;

(3) thirdly, the displacement response calculated by the constant damping model attenuates faster, causing the analysis results may be too small in the seismic analysis of the structure. So the structure designed may be unsafe on this basis;

(4) finally, under biaxial harmonic load, the strength and stiffness degradation of FRP-C RC columns in two bending directions affect each other, which aggravates the decline of their ductility capacity and the seismic capacity will weaken significantly.

In summary, the nonlinear damping model considering the bond slip of reinforcement is adopted for the structure designed will be safer.

Some studies could be carried out in the following aspects: Firstly, the zero-length element model of FRP-confined concrete is improved by conducting bond slip tests of reinforced concrete members in various FRP wrapping forms and establishing corresponding bond slip models; secondly, the cyclic loading and unloading tests of reinforced concrete members with various FRP wrapping forms considering bond-slip effect are carried out to establish the corresponding calculation model.

5. Conclusions

In order to further improve the FRP composite material application in RC structures in seismic design, this paper designed a new train of thought. By introducing zero-length units for reinforcement bond-slip and utilizing regression loss coefficient to redefine the nonlinear damping ratio, we established a nonlinear damping model for FRP-C RC columns considering bond-slip of steel bars, which was successfully used in dynamic response analysis. The conclusions of this study are as follows:

(1) By comparing with the experimental results, the proposed model of FRP-C RC column considering bond-slippage is proved to be reasonable for hysteretic dissipation energy analysis. Additionally, the relative errors of simulation and test results are less than 10%, except for the case of AR-1 specimen with a lateral displacement rate at 0.005, the relative error is 12.05%.

(2) By calculating the hysteretic behavior of the proposed model under horizontal reciprocating loads, the unit energy dissipation regression formula considering steel bars' bond-slip is established, as the Equations (17) and (18).

(3) Based on the complex damping theory, the loss factor expression considering steel bars' bond slip is established, and the damping ratio is redefined.

(4) By calculating the time history responses of FRP-C RC circular and square columns under unidirectional and bidirectional harmonic loads, it can be seen that the column top maximum displacement of the proposed damping model is almost 5%~7% larger than that of the Li's damping model and 15%~21% larger than that of the constant damping model.

Author Contributions: Conceptualization, Y.W. and K.G.; methodology, Y.W. and K.G.; validation, K.G. and Q.G.; investigation, K.G.; resources, K.G. and Q.G.; writing—original draft preparation, K.G. and Q.G.; writing—review and editing, K.G. All authors have read and agreed to the published version of the manuscript.

Funding: This research received no external funding.

Institutional Review Board Statement: Not applicable.

Informed Consent Statement: Not applicable.

Data Availability Statement: No new data were created or analyzed in this study. Data sharing is not applicable to this article.

Conflicts of Interest: The authors declare no conflict of interest.

References

1. Lignola, G.P.; Prota, A.; Manfredi, G. Simplified Modeling of Rectangular Concrete Cross-Sections Confined by External FRP Wrapping. *Polymers* **2014**, *6*, 1187–1206. [CrossRef]
2. Isleem, H.F.; Wang, D.; Wang, Z. Modeling the axial compressive stress-strain behavior of CFRP-confined rectangular RC columns under monotonic and cyclic loading. *Compos. Struct.* **2018**, *185*, 229–240. [CrossRef]
3. Dai, J.-G.; Bai, Y.-L.; Teng, J.G. Behavior and Modeling of Concrete Confined with FRP Composites of Large Deformability. *J. Compos. Constr.* **2011**, *15*, 963–973. [CrossRef]
4. Tabbara, M.; Karam, G. Parametric Investigation of the Effects of Localization and Slenderness on the Stress–Strain Response and Confinement Efficiency in FRP-Wrapped Concrete Cylinders. *Appl. Sci.* **2020**, *10*, 3432. [CrossRef]
5. Uddin, N. *Developments in Fiber-Reinforced Polymer (FRP) Composites for Civil Engineering*; Woodhead Publishing Series in Civil and Structural Engineering: Sawston, UK, 2013.
6. Milani, G.; Shehu, R.; Valente, M. Seismic Upgrading of a Masonry Church with FRP Composites. *Mater. Sci. Forum* **2016**, *866*, 119–123. [CrossRef]
7. Di Ludovico, M.; Prota, A.; Manfredi, G.; Cosenza, E. Seismic strengthening of an under-designed RC structure with FRP. *Earthq. Eng. Struct. Dyn.* **2007**, *37*, 141–162. [CrossRef]
8. Abbassi, M.; Dabbagh, H. Seismic Response of Reactive Powder Concrete Columns Confined with FRP. *Slovak J. Civ. Eng.* **2019**, *27*, 12–20. [CrossRef]
9. Cai, Z.-K.; Wang, D.; Smith, S.T.; Wang, Z. Experimental investigation on the seismic performance of GFRP-wrapped thin-walled steel tube confined RC columns. *Eng. Struct.* **2016**, *110*, 269–280. [CrossRef]

10. Liu, J.; Sheikh, S.A. Fiber-reinforced polymer-confined circular columns under simulated seismic loads. *ACI Struct. J.* **2013**, *110*, 941–951.
11. Wang, D.; Wang, Z.; Smith, S.T.; Yu, T. Seismic performance of CFRP-confined circular high-strength concrete columns with high axial compression ratio. *Constr. Build. Mater.* **2017**, *134*, 91–103. [CrossRef]
12. Liu, X.; Li, Y. Experimental study of seismic behavior of partially corrosion-damaged reinforced concrete columns strengthened with FRP composites with large deformability. *Constr. Build. Mater.* **2018**, *191*, 1071–1081. [CrossRef]
13. Ozbakkaloglu, T.; Lim, J.C. Axial compressive behavior of FRP-confined concrete: Experimental test database and a new design-oriented model. *Compos. Part B Eng.* **2013**, *55*, 607–634. [CrossRef]
14. Lam, L.; Teng, J. Design-oriented stress–strain model for FRP-confined concrete. *Constr. Build. Mater.* **2003**, *17*, 471–489. [CrossRef]
15. Liu, H.Z.; Wang, J.P.; Zhang, Z.M.; Yuan, D.N.; Liu, L.L. Strain-dependent nonlinear damping and application to dynamic analysis of elastic linkage mechanism. *J. Sound Vib.* **2005**, *281*, 399–408. [CrossRef]
16. Ozcan, O.; Binici, B.; Ozcebe, G. Improving seismic performance of deficient reinforced concrete columns using carbon fiber-reinforced polymers. *Eng. Struct.* **2008**, *30*, 1632–1646. [CrossRef]
17. Balsamo, A.; Colombo, A.; Manfredi, G.; Negro, P.; Prota, A. Seismic behavior of a full-scale RC frame repaired using CFRP laminates. *Eng. Struct.* **2005**, *27*, 769–780. [CrossRef]
18. Su, L.; Li, X.; Wang, Y. Experimental study and modelling of CFRP-confined damaged and undamaged square RC columns under cyclic loading. *Steel Compos. Struct.* **2016**, *21*, 411–427. [CrossRef]
19. Yuanfeng, W.; Xiaoran, L. Non-linear damping of FRP-confined damaged reinforced concrete columns. *Eng. Struct.* **2013**, *57*, 289–295. [CrossRef]
20. Li, X.; Wang, Y.; Su, L. Damping determination of FRP-confined reinforced concrete columns. *Comput. Concr.* **2014**, *14*, 163–174. [CrossRef]
21. Zinno, A.; Lignola, G.; Prota, A.; Manfredi, G.; Cosenza, E. Influence of free edge stress concentration on effectiveness of FRP confinement. *Compos. Part B Eng.* **2010**, *41*, 523–532. [CrossRef]
22. Lignola, G.; Prota, A.; Manfredi, G.; Cosenza, E. Non-linear modeling of RC rectangular hollow piers confined with CFRP. *Compos. Struct.* **2009**, *88*, 56–64. [CrossRef]
23. Choi, E.; Cho, B.-S.; Jeon, J.-S.; Yoon, S.-J. Bond behavior of steel deformed bars embedded in concrete confined by FRP wire jackets. *Constr. Build. Mater.* **2014**, *68*, 716–725. [CrossRef]
24. Lignola, G.P.; Nardone, F.; Prota, A.; Manfredi, G. Analytical model for the effective strain in FRP-wrapped circular RC columns. *Compos. Part B Eng.* **2012**, *43*, 3208–3218. [CrossRef]
25. Fernandes, C.; Varum, H.; Costa, A. Importance of the bond–slip mechanism in the numerical simulation of the cyclic response of RC elements with plain reinforcing bars. *Eng. Struct.* **2013**, *56*, 396–406. [CrossRef]
26. Harajli, M.H. Effect of confinement using steel, FRC, or FRP on the bond stress-slip response of steel bars under cyclic loading. *Mater. Struct.* **2006**, *39*, 621–634. [CrossRef]
27. Harajli, M.H. Bond Stress–Slip Model for Steel Bars in Unconfined or Steel, FRC, or FRP Confined Concrete under Cyclic Loading. *J. Struct. Eng.* **2009**, *135*, 509–518. [CrossRef]
28. Verderame, G.M.; Fabbrocino, G.; Manfredi, G. Seismic response of r.c. columns with smooth reinforcement. Part I: Monotonic tests. *Eng. Struct.* **2008**, *30*, 2277–2288. [CrossRef]
29. Verderame, G.M.; Fabbrocino, G.; Manfredi, G. Seismic response of r.c. columns with smooth reinforcement. Part II: Cyclic tests. *Eng. Struct.* **2008**, *30*, 2289–2300. [CrossRef]
30. Sritharan, S.; Priestley, M.N.; Seible, F. Nonlinear finite element analyses of concrete bridge joint systems subjected to seismic actions. *Finite Elements Anal. Des.* **2000**, *36*, 215–233. [CrossRef]
31. Otani, S. Inelastic Analysis of R/C Frame Structures. *J. Struct. Div.* **1974**, *100*, 1433–1449. [CrossRef]
32. Sezen, H.; Setzler, E.J. Reinforcement slip in reinforced concrete columns. *ACI Struct. J.* **2008**, *105*, 280–289.
33. Zhao, J.; Sritharan, S. Modeling of Strain Penetration Effects in Fiber-Based Analysis of Reinforced Concrete Structures. *ACI Struct. J.* **2007**, *104*, 133–141. Available online: https://www.researchgate.net/publication/281456008 (accessed on 2 January 2020).
34. Mazzoni, S.; McKenna, F.; Scott, M.H.; Fenves, G.L. *The Open System for Earthquake Engineering Simulation (OpenSees) User Command-Language Manual*; Pacific Earthquake Engineering Research Center, University of California: Berkeley, CA, USA, 2006.
35. Melo, J.; Fernandes, C.; Varum, H.; Rodrigues, H.; Costa, A.; Arêde, A. Numerical modelling of the cyclic behaviour of RC elements built with plain reinforcing bars. *Eng. Struct.* **2011**, *33*, 273–286. [CrossRef]
36. Scott, B.D.; Park, R.; Priestley, M.J.N. Stress-Strain Behavior of Concrete Confined by Overlapping Hoops at Low and High Strain Rates. *ACI J. Proc.* **1982**, *79*, 13–27. [CrossRef]
37. Karsan, I.D.; Jirsa, J.O. Behavior of Concrete under Compressive Loadings. *J. Struct. Div.* **1969**, *95*, 2543–2564. [CrossRef]
38. Lam, L.; Teng, J.G. Design-Oriented Stress-Strain Model for FRP-Confined Concrete in Rectangular Columns. *J. Reinf. Plast. Compos.* **2003**, *22*, 1149–1186. [CrossRef]
39. Taucer, F.; Spacone, E.; Filippou, F.C. *A Fiber Beam-Column Element for Seismic Response Analysis of Reinforced Concrete Structures*; Earthquake Engineering Research Center, College of Engineering, University of California: Berkeley, CA, USA, 1991.
40. Yoneda, K.; Kawashima, K.; Shoji, G. Seismic retrofit of circular reinforced bridge columns by wrapping of carbon fiber sheets. *Doboku Gakkai Ronbunshu* **2001**, *682*, 41–56. [CrossRef]
41. Lazan, B.J. *Damping of Materials and Members in Structural Mechanics*; Pergamon Press: Oxford, UK; London, UK, 1968.

42. Yu, Q.; Tao, Z. *New Type Composite Structure Column—The Experiment, Theory and Methods*; Science Press: Beijing, China, 2006; pp. 317–351.
43. Li, X.R. Non-Linear Damping Properties and Dynamic Response of FRP-Confined Reinforced Concrete Columns. Ph.D. Thesis, Beijing Jiaotong University, Beijing, China, July 2013.